Available online at www.sciencedirect.com
SCIENCE DIRECT®
Biomass and Bioenergy 27 (2004) 299–312
BIOMASS & BIOENERGY
www.elsevier.com/locate/biombioe

Characterization of laser-induced ignition of biogas–air mixtures

Christian Forsich[a,*], Maximilian Lackner[a], Franz Winter[a], Herbert Kopecek[b], Ernst Wintner[b]

[a] *Institute of Chemical Engineering, Vienna University of Technology, Getreidemarkt 9-166, Wien, A-1060 Austria*
[b] *Institut für Photonik, Technische Universität Wien, Gußhausstraße 25-29, Wien, A-1040 Austria*

Received 31 March 2003; received in revised form 15 September 2003; accepted 12 November 2003

Abstract

Fuel-rich to fuel-lean biogas–air mixtures were ignited by a Nd:YAG laser at initial pressures of up to 3 MPa and compared to the ignition of methane–air mixtures. The investigations were performed in a constant volume vessel heatable up to 473 K. An InGaAsSb/AlGaAsSb quantum well ridge diode laser operating at 2.55 μm was used to track the generation of water in the vicinity of the laser spark in a semi-quantitative manner. Additionally, the flame emissions during the ignition process were recorded and a gas inhomogeneity index was deduced. Laser-induced ignition and its accompanying effects could be characterized on a time scale spanning four orders of magnitude.

The presence of CO_2 in the biogas reduces the burning velocity. The flame emissions result in a much higher intensity for methane than it was the case during biogas ignition. This knowledge concludes that engines fuelled with biogas ultimately affect the performance of the process in a different way than with methane. Methane–air mixtures can be utilized in internal combustion engines with a higher air–fuel ratio than biogas. Comparing failed laser-induced ignition of methane–air and biogas–air mixtures similar results were obtained.

The three parameters water absorbance, flame emission and the gas inhomogeneity index constitute a suitable tool for judging the quality of laser-induced ignition of hydrocarbon–air mixtures at elevated pressures and temperatures as encountered in internal combustion engines.

Keywords: Biogas; Combustion; Laser ignition; Diode laser; In situ; Laser spectroscopy

1. Introduction

In view of the limitation of conventional fossil fuel reserves intensive search for alternative fuels for use in internal combustion engines is going on. Several reports dealing with the utilization of renewable fuels for energy generation are presented in [1–9]. Biogas is CO_2-neutral and can act as a promising alternative fuel having a high availability. The two most common sources of biogas are digester gas and landfill gas. Bacteria form biogas during anaerobic fermentation of organic matters. The degradation is a very complex process and requires certain environmental conditions. Biogas is primarily composed of CH_4 (50–70%) and CO_2 (25–50%). Digester gas is produced at sewage plants during treatment of munic-

* Corresponding author. Tel.: +43-1-58801-159-47; fax: +43-1-58801-159-99.
E-mail address: forsich@mail.zserv.tuwien.ac.at (C. Forsich).

0961-9534/$ - see front matter © 2004 Elsevier Ltd. All rights reserved.
doi:10.1016/j.biombioe.2004.02.002

ipal and industrial sewage. Landfill gas is obtained during decomposition of organic waste in sanitary landfills. In Vienna, such a sanitary landfill is situated at Rautenweg. The obtained biogas is stored and serves as fuel in gas engines to drive a generator producing electricity which is fed into the municipal power supply network. Additionally, thermal energy is generated which is used for heating purposes.

Electric spark plugs are common ignition sources in internal combustion engines. Though spark plug technology is being improved continuously, one can not get rid of some intrinsic drawbacks. Laser sources for initiating combustion have encountered increased interest recently [10–14] because of its many potential benefits over conventional ignition systems. In general, laser ignition is capable of providing multi-point ignition sites [15,16], that can be controlled to ignite a gaseous combustible mixture either sequentially or simultaneously. One of the main advantages is the choice of optimal ignition location which is not easy in conventional ignition systems. Further, precise ignition timing as well as the ignition energy and the deposition rate can be controlled easily. Laser ignition is non-intrusive so that quenching effects on electrodes and walls can be prevented.

In internal combustion engines the air–fuel ratio λ shows a great influence on NO_x-formation in the exhaust gas, leading to reduced NO_x emissions with increasing λ-values due to lower combustion temperatures. On the other side unburned (hydrocarbon) HC-concentration in the exhaust gas have to be considered as well as the thermal efficiency and the power output of the engine when operating in fuel-lean regimes. Too lean fuel–air mixtures cause harsh and irregular running of the engine due to incomplete combustion processes and slow burning velocities, respectively. When using biogas as fuel one must also pay attention to several harmful ingredients such as H_2S polluting the catalytic converter of the engine.

Biogas used for the ignition measurements is provided from the municipal sewage plant in Bad Voeslau, Lower Austria. The composition of biogas varies, depending on the origin. The composition of the biogas used in this work is given in Table 1.

In this work laser ignition of biogas–air mixtures is compared to methane–air mixtures using a spectroscopic technique called tunable diode laser absorption spectroscopy (TDLAS). This technique does not influence the system to be explored and provides in situ data, that is right at the spot. As a consequence, time delays and sampling errors can be avoided.

Table 1
Composition of the biogas used for the investigation of laser-induced ignition (all values ±5%). Nitrogen is the balance

Compounds	Concentration
CH_4	50.5 vol%
CO_2	31.7 vol%
O_2	0.5 vol%
CO	375 vppm
H_2S	80 vppm

2. Theory

Generally, laser radiation interacts with the gas molecules of a combustible mixture via (1) thermal ignition, (2) photochemical ignition, (3) resonant breakdown and (4) non-resonant breakdown [17].

In the laser-induced thermal ignition there is no electrical breakdown. The laser radiation is used to heat up and increase the temperature of the gas.

In photochemical ignition laser photons generally in the UV are absorbed by the target molecules and cause them to dissociate into reactive radicals. If the radical production rate surpasses the recombination rate chain branching reactions lead to ignition and finally to combustion.

In resonant breakdown a target molecule is dissociated by a non-resonant multiphoton dissociation process. The produced atoms are then ionized by a resonant multiphoton ionization process. The electrons generated in this way absorb photons leading to a plasma breakdown.

Non-resonant breakdown is most similar to conventional spark ignition. In laser spark ignition a focused laser beam of irradiance in the order of 10^{10} W/cm^2 is sufficient to generate a plasma spark either by multiphoton ionization or electron cascade process. This ignition mechanism leads to a plasma breakdown and finally to combustion.

Fig. 1 depicts a time scale of the major processes involved in laser-induced ignition which covers several orders of magnitude in time. The ignition process

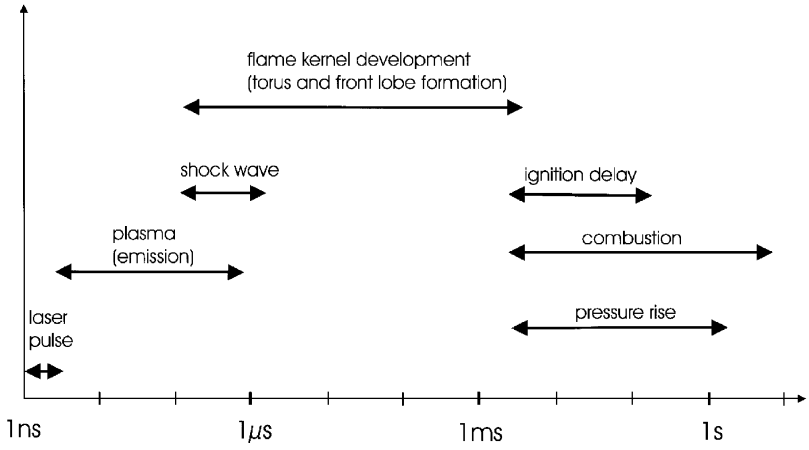

Fig. 1. Time scale of the major processes involved in laser-induced ignition.

starts with the energy deposition of the laser pulse with an irradiance in the order of 10^{10} W/cm^2. Several photons are simultaneously absorbed by a gas molecule or atom leading to ionization if the energy of the photons exceeds the ionization potential. This so called multiphoton ionization generates seed electrons necessary for the following electron cascade process, leading to a plasma formation with high temperature (about 10^6 K) and high pressure (about 10^3 atm) [11]. The high pressure region of the plasma develops to a spherical shock wave. Pressure gradients lead to complex flow patterns and finally vortical motions are developed. These vortical motions are the reason for the development of two distinct flame kernel segments: a torus-like shape propagating radially and a front lobe propagating back toward the laser source. The front lobe formation can be attributed to the asymmetric deposition of laser energy in the direction of the laser [18].

The following ignition delay can be in the order of hundreds of ms depending on the composition of the combustible mixture. During induction time and already during flame kernel development radical chain reactions may take place leading to combustion if the radical production rate surpasses the recombination rate. The combustion process of a fuel-rich mixture lasts about one second for complete combustion in the pressure vessel. Spectroscopic measurements provide information including ignition delay and the combustion process (see Fig. 1). Ignition processes are particularly difficult to investigate, and not yet fully understood because they occur on a short time scale with harsh experimental conditions. Ignition processes are important to understand because slight differences in the early stages of combustion might lead to a significantly different final combustion result. It is therefore of big interest to determine the main characteristics of laser ignition by deploying diagnostic methods working in different time domains. Laser ignition of gases, predominantly methane–air mixtures, has been studied previously [19–23].

In this work, a spectroscopic method is demonstrated tracking the ignition for almost four orders of magnitude in time, starting with ignition and ending after approximately one second with total conversion. Laser spectroscopy is a powerful tool to conduct in situ measurements under harsh environmental conditions (high pressure and temperature) such as in internal combustion engines. The attenuation of the laser light is directly proportional to the concentration of the absorbing species in the limit of uniform temperature and pressure (which poses severe constraints to the interpretation of the spectroscopic signals in these experiments). With I being the intensity of the transmitted light and I_0 being the incident light intensity, one can calculate the absorbance A according to Lambert Beer's law $A = \ln(I_0/I)$. The laser emission wavelength can be tuned by changing the temperature or by varying the injection current. In this work, the laser

frequency was matched to a chosen transition by fixing the temperature and tuning was done by current modulation. This behaviour allows selecting a single rovibrational line of the molecule under investigation that is free from interferences from other species. The laser wavelength was tuned over an entire strong absorption line of water around 2.55 μm. Since water is formed during the early stages of combustion it was chosen as an indicator for the ignition process. In this way one does not only obtain the value of the absorbance at the peak, but also the intensities at its boundaries. Compared to fixed-wavelength methods, this technique known as tunable diode laser absorption spectroscopy (TDLAS) allows to discern resonant absorption from unspecific effects like partial blocking of the beam, scattering or beam steering.

The characterization of laser-induced ignition with various fuel–air ratios was examined evaluating three parameters. These parameters were obtained from spectroscopic measurements of water vapor formed during combustion and are water absorbance, flame emission and gas inhomogeneity index. For further information on the parameters referred to [24].

At 2.55 μm water shows strong absorption lines. The strongest absorption feature is a double peak of water which is situated around 2.55 μm. A calculated reference spectrum of this double peak can be found in [24]. Parameters necessary for this calculation were obtained from the spectroscopic data base HITRAN [25].

The selected absorption feature near 2.55 μm is situated in a continuous tuning range where no mode hops occur.

The evaluation principle of water absorbance is illustrated in Fig. 2. As mentioned above, diode laser can be frequency tuned either by changing the temperature or injection current. The latter was done during the investigations. In Fig. 2a, a linearly increasing current ramp is applied to the semiconductor laser. At the "bend" the laser reaches its threshold and the output power starts to rise linearly with the current. Note that with linearly increasing current simultaneously the emission wavelength changes too. In Fig. 2b, an absorbing species is present in the beam path forming a "dip" in the transmitted detector signal. The trace in Fig. 2a is called baseline or initial laser intensity I_0 and the curve in Fig. 2b is termed transmitted laser intensity I. The absorbance A is obtained by dividing the initial laser intensity I_0 by the transmitted laser intensity I and taking the natural logarithm according to Lambert Beer's law. The absorbance is linearly proportional to the column density (concentration times path length) of the absorbing species. The absorbance is depicted in Fig. 2c.

The second parameter investigating laser-induced ignition was the flame irradiation. This flame emission is the reason for the offset in the recorded detector signal during the measurements. Besides the transmitted laser light additional electromagnetic radiation (visible and infrared) caused by the flame is tracked by the detector. With a detector response from approximately 1–10 μm most of the radiation contributes to the signal.

The third parameter judging the quality of laser-induced ignition is called gas inhomogeneity index. The intensity of laser radiation hitting the detector fluctuates over time which is caused by non-resonant absorption and non-specific beam attenuation, respectively. These unspecific effects result from partial blocking (e.g. due to soot) of the beam, scattering and beam steering due to refractive index gradients. Additionally, the deflections are caused by the plasma and the shock wave influencing the beam path. The variations of the laser intensity were expressed in terms of a frequency [Hz] and the derivation thereof. The reciprocal of the time duration Δt_i times 0.5 was calculated to obtain a frequency f $f_i = (1/\Delta t_i) * 0.5$. The time duration Δt_i is the time span between the ascending ith peak and the descending ith peak. The received frequency was assigned to the mean time $t_{i,m} = (t_i + t_{i+1})/2$. The fluctuations themselves one is not interested in. The aim is to obtain alterations of the transmitted signal. Therefore, the derivation D of the frequency f was carried out according to $D = \mathrm{d}f/\mathrm{d}t \sim \Delta f/\Delta t = (f_{i+1} - f_i)/(t_{i+1,m} - t_{i,m})$. The result is the introduction of the third parameter called gas inhomogeneity index [s^{-2}].

In Fig. 3, one can see schematically how information on ignition is obtained.

In Fig. 3a, the original data of an ignition test run are shown. Each of the consecutive triangles, as highlighted in Fig. 2, is a single measurement. In Fig. 3b, the offset has been subtracted. The offset is caused by thermal radiation of the heated reactor walls (constant part) and the infrared emissions of the flame (convex part). One can see that the triangles do not

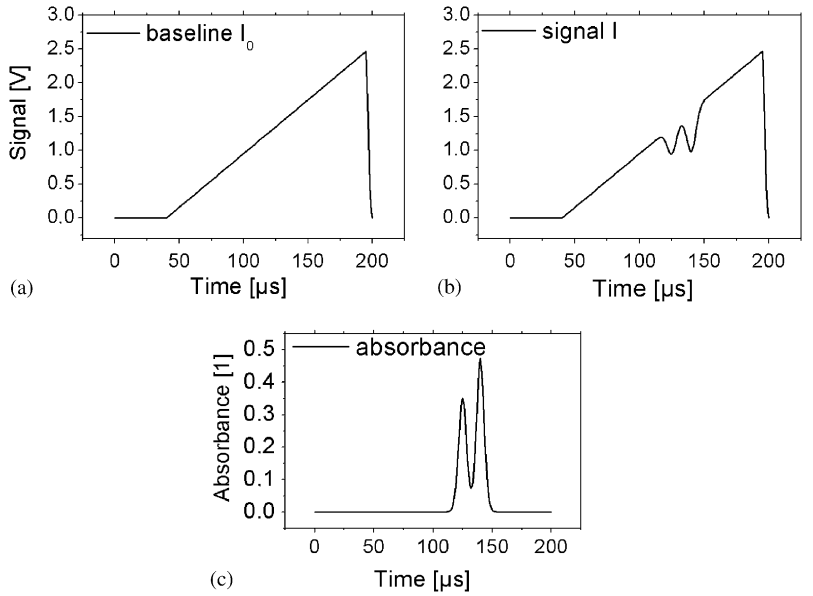

Fig. 2. Determination of the absorbance in tunable diode laser absorption spectroscopy: (a) The laser output power as a function of current. The injection current linearly increases, simultaneously the emission wavelength changes. The trace represents the baseline I_0 when no absorber is present. (b) The same situation with an absorbing species in the beam path, resulting in a dip of the signal I is depicted. (c) The absorbance calculated as $\ln(I_0/I)$. The absorbance is directly proportional to the concentration of absorbing species.

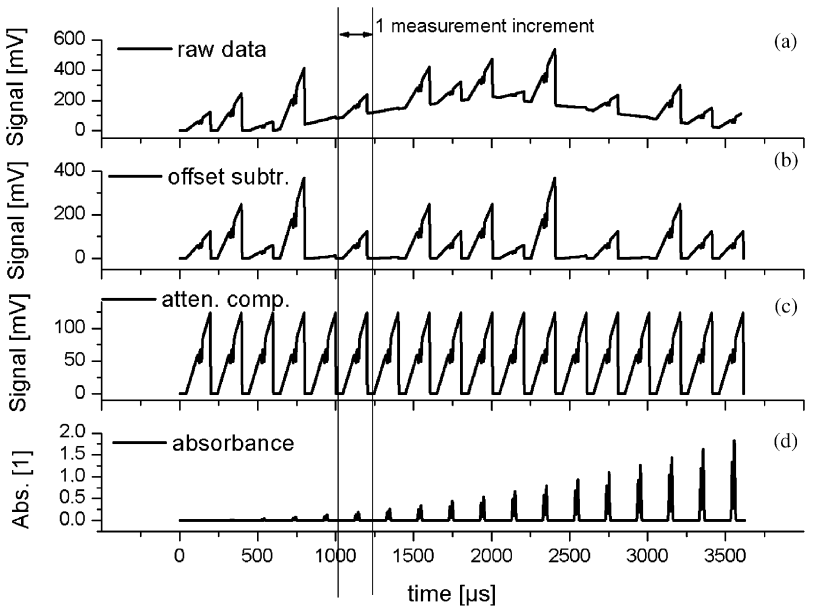

Fig. 3. (a)–(d)Scheme of obtaining the absorbance of water vapor generated close to the location of the laser spark. Additional information was obtained from the flame emission and the fluctuations of the transmission.

possess the same signal height. This fluctuation is due to non-specific beam attenuation. In Fig. 3c, this was compensated. Finally in Fig. 3d, the absorbance deduced from the absorption peak (compare Fig. 2) is shown. The core information is in the increasing water concentration (the absorbance at the resonance wavelength). The offset, viz. the emissions of the flame, was used to gain additional information. So were the fluctuations of the transmission as shown in Fig. 3b in terms of the height of the triangular curves. As a result the gas inhomogeneity index was introduced. Note that in Fig. 3, there are only a few triangular current ramps. In order to correctly probe the system, the time scale of these ramps must be shorter than the time scale of the experimental noise.

The spectroscopic measurements were performed with a repetition rate of 5 kHz, corresponding to a time resolution of 0.2 ms. In other words, the applied laser ramps scanning over an entire absorption feature of water vapor around 2.55 μm had a time span of 0.2 ms each.

Processes involved in laser-induced ignition occur on different time scales (see Fig. 1). The energy deposition happens within 5–10 ns, plasma generation and the following shock wave formation lasts about 1 μs. The ignition delay is situated in the ms regime, approximately 10–100 ms, combustion itself lasts about several 100 ms to seconds, depending on the air–fuel ratio of the mixture. The spectroscopic technique used for the investigation of laser-induced ignition is able to track the ignition process over more than four orders of magnitude in time.

3. Experimental

The experimental setup used for the research experiments is shown in Fig. 4. Detailed information concerning the ignition laser and the optical setup can be found in [22]. The pressure vessel is constructed to withstand pressures up to 30 MPa. Since there is a factor of about 7 between the initial pressure and maximum combustion pressure, the ignition of gas mixtures can be investigated up to 4 MPa filling pressure. This is particularly important because in stationary gas engines, pressures are in the order of this magnitude.

The cylindrical combustion chamber of 9×10^{-4} m^3 volume is composed of a metallic tube made of refractory steel (internal length 0.223 m, internal diameter 0.0716 m). The combustion vessel is heated by heating rods situated outside the metal cylinder able to operate between room temperature and up to 473 K. To allow surpassing either the ignition laser beam and the semiconductor laser the chamber is mounted with 4 windows of sapphire glass. Two windows located on the transverse opposite sides of the chamber admit the laser beam for the ignition process, while the other two, situated in the longitudinal direction on opposite sides, serve as the entrance and exit windows for the laser beam of the spectroscopic device. The cell has several ports around its periphery. As mentioned before 4 ports were equipped with entrance and exit windows. The other ports were used for gas inlets, gas outlet and for mounting a pressure sensor. This piezoelectric pressure sensor is utilized in combination with a charge amplifier to determine the pressure inside the chamber. The pressure trace was recorded on an oscilloscope (100 MHz, 1GS/s) and read from an interface into a personal computer. A Q-switched Nd-YAG laser (Quantel Brilliant) operating at 1064 nm and a pulse duration of 5 ns is focused into the combustion chamber to initiate ignition. The laser energy can be attenuated using a polarizer from 50 to 1 mJ per pulse.

An InGaAsSb/AlGaAsSb quantum well ridge diode laser tunable around 2.55 μm was employed to track the generation of water close to the ignition spark. The

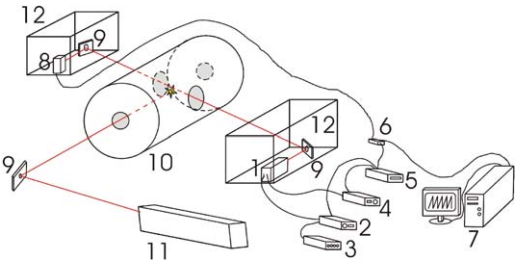

Fig. 4. Schematic diagram of the experimental setup. The laser-induced ignition tests were performed in a constant volume vessel equipped with 4 windows. The spectroscopic laser device was sent through the pressurized combustion vessel perpendicularly to the igniting laser beam (Nd:YAG laser, 5 ns pulse duration) close to the ignition spark. 1: diode laser at 2.55 μm; 2: laser driver; 3: function generator; 4: temperature controller; 5: 15 V power supply; 6: amplifier; 7: PC with data acquisition card; 8: detector; 9: mirror; 10: pressurized combustion vessel; 11: pulsed Nd:YAG laser; 12: N_2-purged boxes.

spectroscopic device was thermo-stated at 289 K using a laser diode temperature controller in conjunction with a peltier element and a NTC temperature sensor. The laser was frequency tuned utilizing a laser driver. A voltage ramp of 0–4 V with a repetition rate of 5 kHz was applied to the laser driver utilizing a function generator. There is a slow rise from 0 to 4 V and a steep decrease to 0 again. One entire sweep is achieved in 1/5000 s, accordingly one scan takes 0.2 ms, thus a time resolution of 0.2 ms can be obtained. Corresponding to the voltage function the laser driver tuned the laser by varying the injection current between 0 and 176 mA while keeping the temperature of the heat sink constant at 289 K.

The laser driver and temperature controller were fed by a 15 V current source protected against the line voltage. An anti-reflection coated plano-convex lens (focal length 5 mm) was utilized to collimate the laser beam. The two boxes containing the semiconductor laser and the spectroscopic setup situated on both sides of the combustion reactor had to be purged with nitrogen to remove the water vapor of the ambient atmosphere (0.5–1 vol%) along the path length to detect the very small amount of water comparatively generated during the combustion process. An infrared photo detector cooled by liquid nitrogen was utilized to track the transmitted laser radiation. The signal of the detector was amplified and visualized on the oscilloscope. The detector signal was transferred to a personal computer and digitized using a high speed data acquisition board.

All experiments were carried out at elevated pressures up to 3 MPa and temperatures up to 473 K to prevent condensation of water on the inner surface of the chamber and especially windows. Fuel (methane, biogas) and pressurized air (standard technical purity) from pressurized gas bottles were delivered automatically to the ignition cell using a gas handling system. Before each ignition event, the combustion cell was first evacuated and purged with air to remove all residual products of the previous combustions. For achieving the desired fuel to air ratio the partial pressure method was used. To prevent spacial inhomogeneity the calculated partial pressure of the fuel was filled first and the fuel pressure inside the ignition cell was monitored using a high resolution pressure meter. Next, air was injected and in this way, the homogeneity was achieved easily by the turbulence of the incoming air stream. The mixture inside the cell was left to stabilize before igniting. The trigger signal provided by the flash lamps of the Nd:YAG laser was used to start the data acquisition.

The investigated methane–air and biogas–air mixtures contained similar methane concentrations but in the case of biogas additionally CO_2 was present.

4. Results and discussion

4.1. Fuel-rich ignition

In this work a tunable diode laser was utilized to characterize laser-induced ignition of biogas–air and methane–air mixtures by evaluating three parameters. The laser beam traversed the combustion vessel in the vicinity of the plasma spark which was generated by a Nd:YAG-laser to ignite the hydrocarbon–air mixtures.

The spectroscopic data of water vapor were used to judge the quality of ignited hydrocarbon–air mixtures by a laser source. In Fig. 5, a typical detector signal of a fuel-rich biogas–air mixture is depicted with a recording time of 261 ms. Due to the effects of severe pressure broadening at high pressures and the ignorance of the exact temperature distribution after ignition, water absorbance could only be determined in a

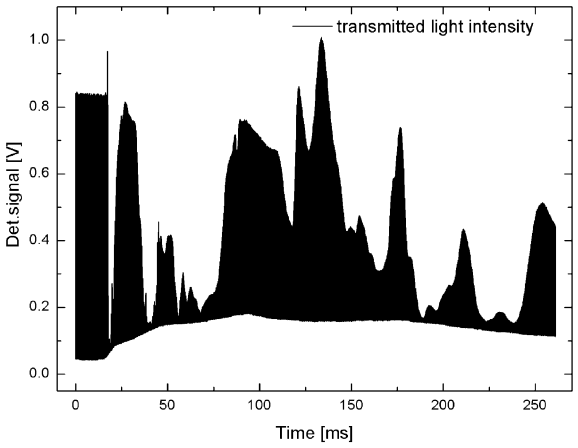

Fig. 5. Original data (detector signal) obtained during laser-induced ignition of a fuel-rich biogas–air mixture (air–fuel ratio λ 0.76; initial filling pressure 3 MPa; temperature 473 K) with a 5 kHz repetition rate, corresponding to a time resolution of 0.2 ms. The transmitted laser light intensity fluctuates over time.

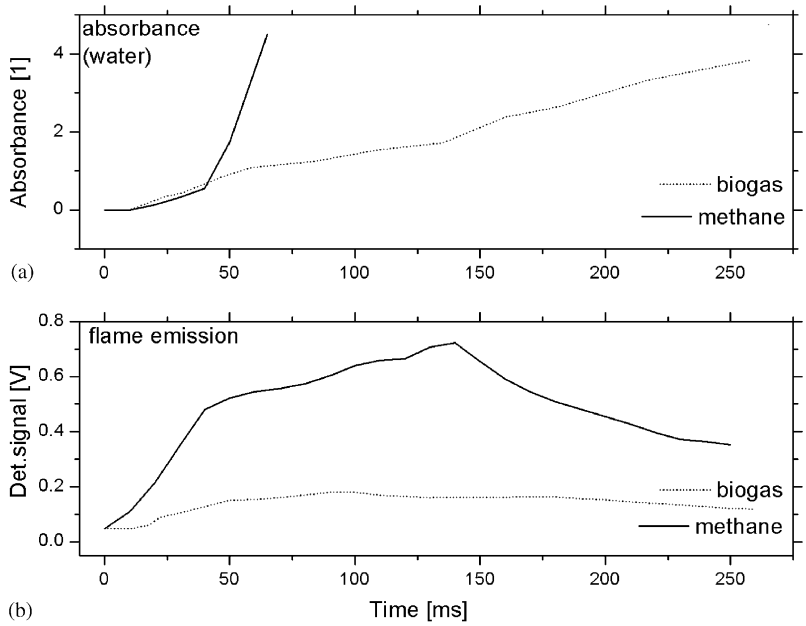

Fig. 6. Evaluated water absorbance and flame emission of the fuel-rich biogas–air mixture depicted in Fig. 5. Comparison with a methane–air mixture of similar composition (air–fuel ratio 0.82; initial filling pressure 3 MPa; temperature 473 K): (a) the water absorbance of methane rises faster than biogas due to CO_2 decelerating the combustion process; (b) the flame emission intensity of a methane–air mixture is by a factor 3 higher compared to biogas.

semi-quantitative manner. For further information the reader is referred to [24]. In this way, one obtains the first characterizing parameter the water absorbance. The flame emission was also evaluated, obtaining the second parameter. A third parameter called gas inhomogeneity index was also introduced.

Fig. 6 depicts the absorbance and the flame emission evaluated from the original data in Fig. 5. Additionally the parameters for the methane–air mixture are included. For the fuel-rich combustion process of biogas the water absorbance rises due to water production during the combustion process and reaches an absorbance of four within 250 ms (Fig. 6a). In this work the absorbance of water vapor was evaluated up to four. Without any sophisticated detection schemes, absorbance above four becomes difficult to measure, since the transmission approaches zero (an absorbance of four corresponds to a transmission of approximately 1.8%). The flame emission rises after approximately 15 ms and reaches a maximum after 100 ms and falls off again (Fig. 6b). The time span of 15 ms at the beginning of ignition is the ignition delay which can be easily deducted from the flame emission parameter.

In a fuel-rich methane–air mixture the water absorbance at 2.55 μm increases faster with time. After approximately 70 ms, it reached already a value of four (1.8% transmittance) which imply an accelerated combustion process compared to biogas–air mixtures (Fig. 6a). The maximum of the flame emission intensity in the rich methane mixture is by factor of 3 higher than for fuel-rich biogas ignition and there is no significant ignition delay (Fig. 6b). The reason for these results could be the presence of CO_2, an incombustible diluent gas in the biogas which reduces the burning velocity due to obstructing the flame propagation during combustion. In comparison to a pure nitrogen diluent, CO_2 is a heat sink, on the basis of its significantly larger heat capacity [Nitrogen: 29.12 J K^{-1} mol^{-1} (298 K); Oxygen: 29.38 J K^{-1} mol^{-1} (298 K); Carbon dioxide: 37.13 J K^{-1} mol^{-1} (298 K); Methane: 35.65 J K^{-1} mol^{-1} (298 K)]. Consequently, the biogas–air flames are cooler and propagate more slowly than the corresponding methane–air flames.

As mentioned before the gas inhomogeneity index was obtained by evaluating the fluctuations of the

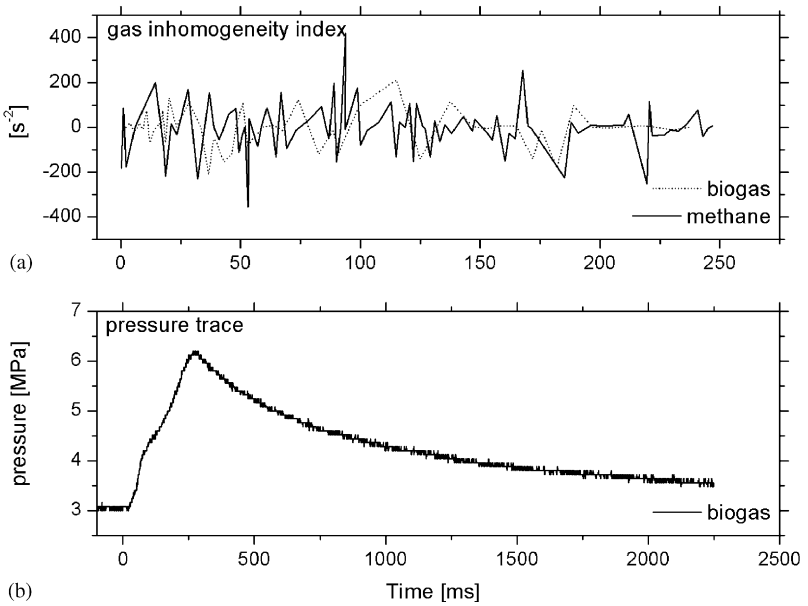

Fig. 7. Gas inhomogeneity index and pressure trace of the fuel–rich biogas–air mixture: (a) depicts the inhomogeneity index of biogas and methane; (b) the corresponding pressure trace of the fuel-rich biogas–air mixture is shown.

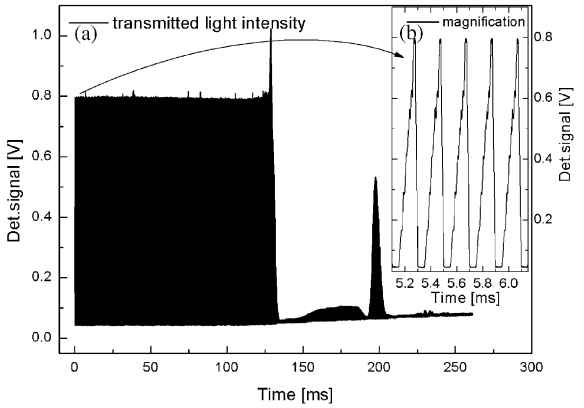

Fig. 8. Original data (detector signal) obtained during laser-induced ignition of a fuel-lean biogas–air mixture (air–fuel ratio λ 1.21; initial filling pressure 3 MPa; temperature 473 K). The inset (b) shows the magnification of the applied laser ramps with a time resolution of 0.2 ms.

transmitted signal. After the ignition delay strong fluctuations are obtained during the whole combustion process as shown in Fig. 7a. The plasma spark ignites the fuel-rich biogas–air mixture and the flame front starts to expand with a high velocity causing irregular transmission variations. The flame front generates temperature gradients which further lead to refractive index gradients inside the pressure vessel. These refractive index gradients partly prevent the laser light falling onto the detector due to deflection and beam steering. The beam can also be partially blocked, e.g. by soot particles but the effect of the refractive index gradients is dominant. The gas inhomogeneity index of biogas does not depict significant differences to a methane–air mixture. In Fig. 7b the pressure rise in the vessel after ignition of a biogas–air mixture is illustrated. The maximum pressure rise is reached after approximately 300 ms and decreases again due to heat losses at the chamber walls. In fuel-rich methane –air mixtures with similar air–fuel ratio the pressure trace rises faster and reaches higher pressures because of the absence of CO_2 resulting in a higher efficiency and power output.

4.2. Fuel-lean ignition

Comparing a fuel-rich biogas–air mixture with a fuel-lean one several differences can be observed. Fig. 8 shows the raw data obtained from a fuel-lean

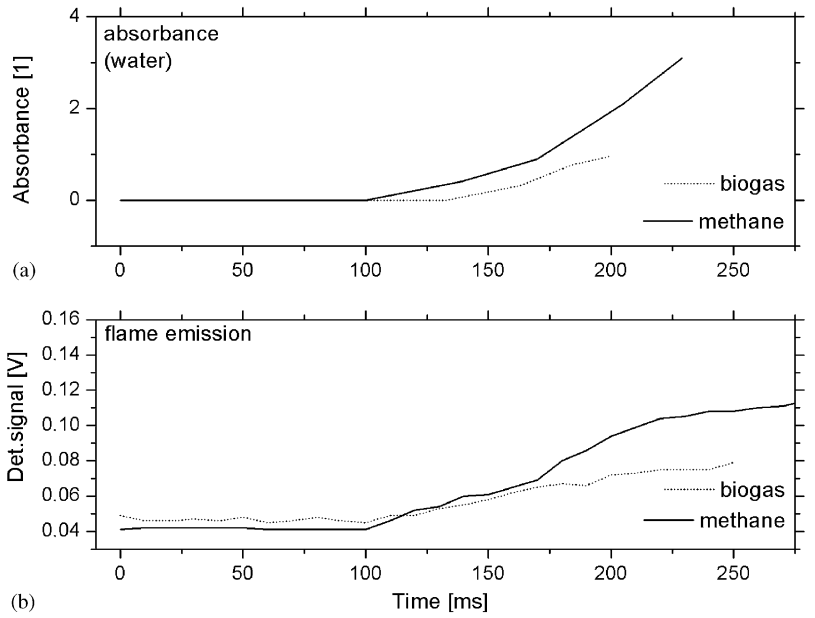

Fig. 9. Evaluated water absorbance and flame emission of the fuel-lean biogas–air mixture depicted in Fig. 8. Comparison with a methane –air mixture of similar composition (air–fuel ratio λ 1.31; initial filling pressure 3 MPa; temperature 473 K): (a) the water absorbance of methane rises faster than biogas due to CO_2 decelerating the combustion process; (b) the flame emission intensity of a biogas–air mixture is compared with a mixture of methane.

biogas–air mixture. In Fig. 8b an inset is shown where one can see the individual ramps applied to the laser. The corresponding characterization parameters are depicted in Figs. 9 and 10. Considering the absorbance the combustion process is decelerated resulting in a reduced water generation. In the fuel-rich mixture water absorbance of 2 (corresponds to a transmission of 13.5%) is reached after approximately 125 ms, whereas in the fuel-lean case the same value is not even obtained after 200 ms as shown in Fig. 9a. In a fuel-lean methane–air mixture a steeper rise of the water absorbance is obtained which corresponds to a faster combustion process.

With regard to the flame emission signal in Fig. 9b an ignition delay time of about 130 ms is reached prior the combustion process is initiated. The slow rise and the lower intensity of the flame emission compared to methane–air mixtures concludes a slow and incomplete combustion of the biogas–air mixture which is also consistent with the slight increase of the water absorbance.

During the ignition delay initiation reactions take place, generating mainly reactive methyl radicals, followed by chain propagation, chain branching and recombination processes. The main initiation steps converting methane to methyl radicals are depicted by the following reactions (R.1–R.3):

$$CH_4 + H \leftrightarrow CH_3 + H_2, \quad (R.1)$$

$$CH_4 + O \leftrightarrow CH_3 + OH, \quad (R.2)$$

$$CH_4 + OH \leftrightarrow CH_3 + H_2O. \quad (R.3)$$

If the radical production rate surpasses the recombination rate chain branching reactions lead to ignition and finally to combustion. During the long ignition delay time of the fuel-lean biogas–air mixture no variations of the transmitted laser signal are apparent because the flame kernel refracting the laser beam is generated at the end of the induction time. The laser signal within the induction time verifies that the homogeneity of the gas phase is ensured.

As shown in Fig. 10a, only slight fluctuations of the gas inhomogeneity index are present because the flame front propagates with decelerated velocity into the unburned mixture influencing the beam path of

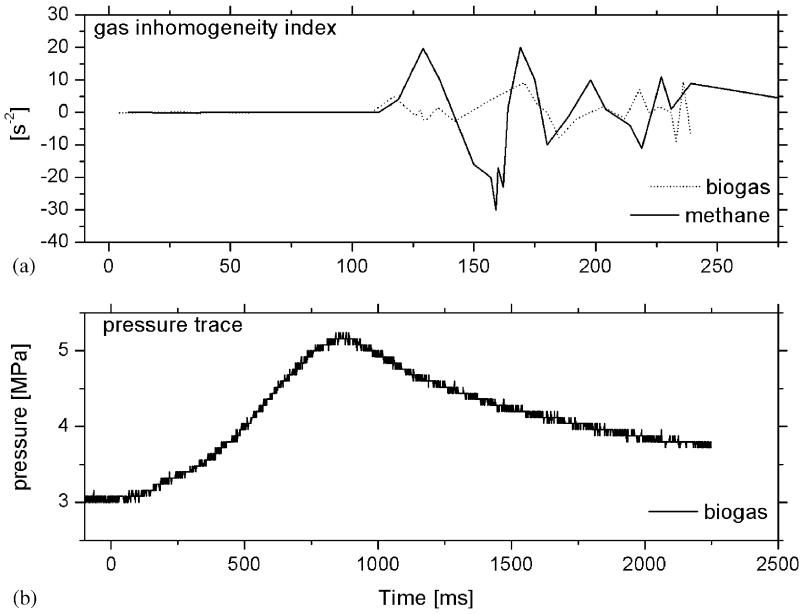

Fig. 10. Gas inhomogeneity index and pressure trace of the fuel-lean biogas–air mixture: (a) depicts the inhomogeneity index of biogas and methane; (b) the corresponding pressure trace of the fuel-lean biogas–air mixture is shown. The peak pressure is lower and reached later compared to the fuel-rich case.

the laser. In Fig. 10b, the recorded pressure trace of the fuel-lean biogas–air mixture is shown. The pressure curve demonstrates a lower and later peak pressure compared to the fuel-rich case in Fig. 7b. During laser-induced ignition of a fuel-lean methane–air mixture the corresponding pressure trace shows again an accelerated combustion process and higher peak pressures and consequently higher temperatures.

Fuel-rich methane–air mixtures show a higher burning velocity than fuel-rich biogas–air mixtures due to the incombustible gas CO_2. The same results are obtained for fuel-lean mixtures. The maximum burning velocity of a mixture is slightly towards the rich side of stoichiometric. By changing the mixture composition into fuel-rich or fuel-lean regions a decrease is observed. Below a certain burning velocity the flame extinguishes and the ignition of the mixture is not possible. Methane–air mixtures are able to run an internal combustion engine (e.g. gas engine) with a higher air–fuel ratio than biogas.

Fuel-lean combustion results in lower peak temperatures and hence reduced NO_x emissions. In contrast, the total unburned hydrocarbon emissions increase. Therefore a kind of compromise has to be found. A problem with fuel-lean mixtures is a reduced burning velocity resulting in a harsh and irregular running of the engine. Multi-point ignition becomes necessary to compensate the loss in flame speed. With multi-point ignition, the distance over which the flame must sweep to complete the combustion process is shortened. The combustion times are, therefore, reduced. Because the combustion times are short, the flame does not have enough time to lose heat resulting in higher combustion temperature and pressure leading to a better thermal efficiency and increased power output.

4.3. Failed ignition

Besides characterizing ignited biogas–air mixtures the evaluated parameters are also able to investigate failed ignition processes. Fig. 11 shows a recorded detector signal and Fig. 12 the corresponding evaluated parameters of a measurement without igniting the mixture. A remarkable dip in the raw data signal at the beginning of the failed ignition event is depicted in Fig. 11. The transmission of the laser beam steeply

decreases and increases again turning into uniform values after approximately 20 ms. Considering the corresponding gas inhomogeneity index in Fig. 12c this effect results in a significant variation in the transmitted laser signal. The remarkable fluctuation at the beginning of the ignition experiment occurs due to the finite dissipation time of the strong thermal gradients induced by the short-lived plasma. This plasma spark [11] is a hot spot with temperatures in the order of 10^6 K and about 2 mm in diameter which serves as a kind of lens refracting the optical beam path of the laser source. Though the plasma spark has a lifetime of several μs it affects the laser beam up to the ms regime. Due to an unsuccessful ignition no water absorbance and flame emission respectively were detected.

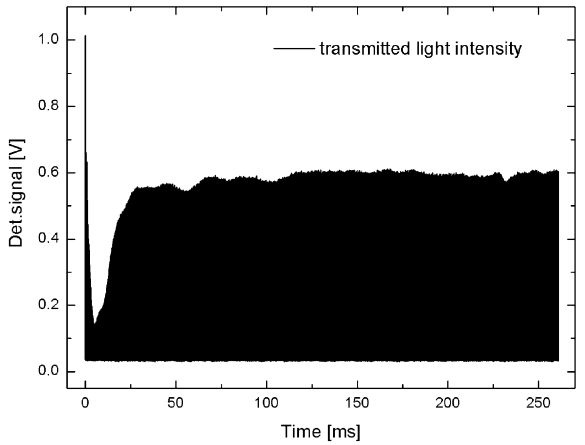

Fig. 11. Original data (detector signal) obtained during failed laser-induced ignition measurement. Parameters: air–fuel ratio λ 1.82; initial filling pressure 3 MPa; temperature 473 K (beyond limit of flammability).

The characteristic dip in transmission of the laser beam due to the effect of the plasma spark could also be observed for a failed methane–air mixture with an air–fuel ratio λ of 2.5. The energy content of the laser pulse was too low to set the mixture on fire and further the generated plasma extinguished. The temperature gradient of the plasma spark deflected the laser beam from the detector causing the marked dip downwards in the laser signal within the first 25 ms of the measurement. The detector signal and the parameters are illustrated in [24].

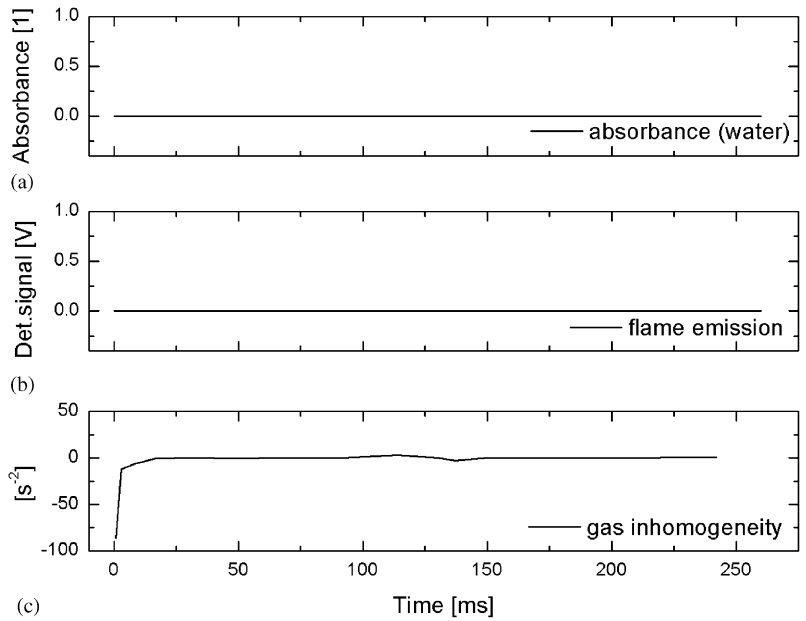

Fig. 12. Characterization parameters obtained from the fuel-lean biogas–air mixture in Fig. 11, namely water absorbance (a), flame emission (b) and the gas inhomogeneity index (c) (derivation of the frequency of the fluctuating transmittance).

5. Conclusions

A spectroscopic technique utilizing a semiconductor laser devise emitting at 2.55 μm was employed to characterize laser-induced ignition of hydrocarbon –air mixtures including biogas and methane as fuels. Three parameters were evaluated from the spectroscopic data, namely the water absorbance, flame emission and the so called gas inhomogeneity index. The in situ laser measurements were performed in a pressurized combustion vessel at initial pressures up to 3 MPa and 473 K.

For combustion processes in engines fuel-lean mixtures are desirable due to lower combustion temperatures leading to reduced NO_x emissions. It is very important to know the lean ignition limit of the fuel used. Biogas–air mixtures show a slower combustion process compared with methane–air mixtures. Because of the lower burning velocity of biogas–air mixtures methane–air mixtures are able to run an internal combustion engine (e.g. gas engine) with a higher air–fuel ratio.

In the fuel-rich case methane–air mixtures reached a water absorbance of four within 70 ms whereas the time for biogas–air mixtures reaching the same value lasted approximately 3 times longer. The maximum of the flame emission intensity in the rich methane mixture is by a factor of 3 higher than for fuel-rich biogas ignition and there is no ignition delay. Fuel-lean biogas–air mixtures exhibit a slower combustion process resulting in lower peak pressure and flame emission compared to methane–air mixtures of similar air–fuel ratio.

The reason for these results could be due to the presence of CO_2 in the biogas which reduces the burning velocity due to obstructing the flame propagation during combustion. CO_2 serves as a heat sink, having a larger heat capacity than nitrogen. Consequently the biogas–air flames are cooler and propagate more slowly than the corresponding methane –air flames. Comparing failed ignition measurements of biogas and methane similar results were obtained. The plasma spark of the laser included insufficient energy to ignite the mixture but generated thermal gradients deflecting the spectroscopic laser beam causing fluctuations of the transmitted laser signal.

Acknowledgements

We gratefully thank Mr. Stocker from LMF (Leobersdorfer Maschinenfabrik) AG, A-2544 Leobersdorf, Austria, for obtaining the biogas.

This work was supported by the Austrian Industrial Research Promotion Fund (FFF) under Grant FFF 803050. We are also indebted to our industrial partner Jenbacher Zuendsysteme GmbH, especially Dr. Guenther Herdin and DI Johann Klausner, for financial and technical support.

References

[1] Chiaramonti D, Bonini M, Fratini E, Tondi G, Gartner K, Bridgwater AV, et al. Development of emulsions from biomass pyrolysis liquid and diesel and their use in engines —Part 1: emulsion production. Biomass and Bioenergy 2003;25(1):85–99.

[2] Chiaramonti D, Bonini M, Fratini E, Tondi G, Gartner K, Bridgwater AV, et al. Development of emulsions from biomass pyrolysis liquid and diesel and their use in engines —Part 2: tests in diesel engines. Biomass and Bioenergy 2003;25(1):101–11.

[3] Rubab S, Kandpal C. A methodology for financial evaluation of biogas technology in India using cost functions. Biomass and Bioenergy 1996;10(1):11–23.

[4] Van den Broek R, Faaij A, Van Wijk A. Biomass combustion for power generation. Biomass and Bioenergy 1996;11(4): 271–81.

[5] Yoshida Y, Dowaki K, Matsumura Y, Matsuhashi R, Li D, Ishitani H, et al. Comprehensive comparison of efficiency and CO_2 emissions between biomass energy conversion technologies—position of supercritical water gasification in biomass technologies. Biomass and Bioenergy 2003;25(3):257–72.

[6] Omer AM, Fadalla Y. Biogas energy technology in Sudan. Renewable Energy 2003;28:499–507.

[7] Kaygusuz K, Türker MF. Biomass energy potential in Turkey. Renewable Energy 2002;26:661–78.

[8] Akinbami JFK, Ilori MO, Oyebisi TO, Akinwumi IO, Adeoti O. Biogas energy use in Nigeria: current status, future prospects and policy implications. Renewable and Sustainable Energy Reviews 2001;5:97–112.

[9] Ni JQ, Nyns EJ. New concept for the evaluation of rural biogas management in developing countries. Energy Conversion and Management 1996;37(10):1525–34.

[10] Phuoc Tran X, White CM, McNeill DH. Laser spark ignition of a jet diffusion flame. Optics and Lasers in Engineering 2002;38:217–32.

[11] Phuoc TX. Laser spark ignition: experimental determination of laser-induced breakdown thresholds of combustion gases. Optics Communications 2000;175:419–23.

[12] Morsy MH, Ko YS, Chung SH. Laser-induced ignition using a conical cavity in CH_4–air mixtures. Combustion and Flame 1999;119:473–82.
[13] Ma JX, Alexander DR, Poulain DE. Laser spark ignition and combustion characteristics of methane–air mixtures. Combustion and Flame 1998;112:492–506.
[14] Phuoc TX, White F. Laser-induced spark ignition of CH_4–air mixtures. Combustion and Flame 1999;119: 203–16.
[15] Morsy MH, Ko YS, Chung SH, Cho P. Laser-induced two-point ignition of premixture with a single-shot laser. Combustion and Flame 2001;125:724–7.
[16] Phuoc TX. Single-point versus multi-point laser ignition: experimental measurements of combustion times and pressures. Combustion and Flame 2000;122:508–10.
[17] Ronney PD. Laser versus conventional ignition of flames. Optical Engineering 1994;33:510–21.
[18] Morsy MH, Chung SH. Numerical simulation of front lobe formation in laser-induced spark ignition of CH_4/air mixtures. 29th International Symposium on Combustion, Sapporo, Japan, 2002.
[19] Kopecek H, Charareh S, Lackner M, Forsich C, Winter F, Wintner E. Laser ignition of methane–air mixtures at high pressures and diagnostics. ASME, Salzburg, Austria, May 11–14, 2003.
[20] Kopecek H, Lackner M, Winter F, Wintner E. Laser ignition of methane–air mixtures at pressures up to 4 MPa. Journal of Laser Physics 2003;13(11):1365.
[21] Kopecek H, Lackner M, Iskra K, Forsich Ch, Rüdisser D, Neger T, et al. Laser ignition of methane–air mixtures at high pressures and optical diagnostics. Proceedings of the SPIE, 2002.
[22] Kopecek H, Maier H, Reider G, Winter F, Wintner E. Laser ignition of methane–air mixtures at high pressures. Experimental Thermal and Fluid Science 2003;27(4): 499–503.
[23] Lackner M, Winter F. What is laser ignition? Combustion file 268, IFRF (International Flame Research Foundation) Online Combustion Handbook 2004, ISSN 1607–9116.
[24] Lackner M, Forsich Ch, Winter F, Kopecek H, Wintner E. In situ Investigation of Laser-Induced Ignition and the Early Stages of Methane–Air Combustion at High Pressures Using a Rapidly Tuned Diode Laser at 2.55 μm. Spectrochimica Acta A: Molecular & Biomolecular Spectroscopy 2003;59(13):2997–3018.
[25] Rothman LS, Rinsland CP, Goldman A, Massie ST, vEdwards DP, Flaud JM, et al. The HITRAN Molecular Spectroscopic Database and HAWKS (HITRAN Atmospheric Workstation). 1996 ed. Journal of Quantitative Spectroscopy & Radiative Transfer 1998;60:665.